

## **Supplemental Data**

### **Phosphatidylinositol-(4,5)-Bisphosphate**

### **Regulates Sorting Signal Recognition by the**

### **Cathrin-Associated Adaptor Complex AP2**

**Stefan Höning, Doris Ricotta, Michael Krauss, Kira Späte, Barbara Spolaore, Alison Motley, Margaret Robinson, Carol Robinson, Volker Haucke, and David Owen**

#### **Supplemental Experimental Procedures**

##### **Mass spectrometry materials and methods**

##### **Sample preparation and tryptic digestion of the phosphorylated and non-phosphorylated AP2 complex for mass spectrometry.**

AP2 samples were stored at 4°C and buffer-exchanged twice with 200 mM ammonium acetate, pH 7.5 using microcentrifuge columns (Micro Bio-spin 6, Bio-Rad) before analysis. Buffer exchange and sample introduction were conducted at room temperature. Dissociation of the complex was performed by treating the sample in 200 mM ammonium acetate at pH 7.5 with a cation exchange matrix (AG 50W-X8 matrix, Bio-Rad). This treatment effectively reduces the pH to between 2 and 3 and this causes the subunits to dissociate. Tryptic digestion was performed on samples of phosphorylated and non-phosphorylated AP2 buffer exchanged to 200 mM ammonium acetate, pH 7.5 and at a complex concentration of 1.5-2.0 mg/ml, estimated by measuring the absorbance at 280 nm. Proteolysis was initiated by adding a stock solution of bovine pancreatic trypsin at a protein/enzyme ratio of 1/50 by weight. The digestions were performed at 37°C in a thermostated bath and stopped after 1 hour by dilution of aliquots of the reaction mixture 2-fold with a solution of 3% acetic acid in acetonitrile.

##### **Nano-electrospray mass spectrometry.**

Mass spectra were acquired on a LCT (Micromass, UK) and on a tandem mass spectrometer Q-TOF 2 (Micromass, UK) modified for high mass operation (Sobott et al 2002) and equipped with a Z-spray nanoflow electrospray interface. Nano-ESI capillaries were prepared in house from borosilicate glass tubes of 1 mm OD and 0.78 mm ID (Harvard Apparatus, Holliston, MA, USA) using a Flaming/Brown P-97 micropipette puller (Sutter Instruments, Hercules, CA, USA), and gold coated using a SEM sputter coater (Polaron, Newhaven, UK). The capillary tips were cut under a stereomicroscope to give inner diameters of 1-5 µm, and typically 0.5-2 µl of solution were loaded for sampling. For the analysis of the intact AP2 complex, pressures and accelerating voltages in the Q-TOF 2 mass spectrometer were adjusted to preserve non-covalent interactions. The following experimental parameters were typically used (positive ion mode): capillary voltage, 1.8 kV; sample cone, 200 V; extractor cone, 100 V; collision energy, 4 V; ion transfer stage pressure  $3.2 \times 10^{-3}$  mbar; quadrupole analyser pressure,  $1.8 \times 10^{-5}$  mbar; TOF analyser pressure,  $4.7 \times 10^{-7}$  mbar; and spectrum acquisition frequency, 3.9 kHz. Analysis of the tryptic digest and MS/MS experiments were performed under the same pressure conditions as above but using a capillary voltage of 1.5 kV, a sample cone of 80 V and an extractor cone set to 0 V. No heating was applied in the electrospray source. For MS/MS, the quadrupole resolution was set to transmit a mass window of ~1 Th for parent ion selection. The collision gas used was argon at an indicated inlet pressure of 30 psi and the collision energy setting was 35 V.

Spectra of the dissociated AP2 complex were acquired on the LCT (Micromass, UK) using a capillary voltage of 1.3 kV, a sample cone of 40 V and an extractor of 3 V, whereas pressure values were at base condition (1.89 mbar in the ion transfer stage pressure and  $7.38 \times 10^{-7}$  mbar as TOF analyser pressure). In both instruments external calibration was performed using a solution of cesium iodide. Instrument control and data acquisition and processing were achieved with MassLynx software (Micromass, UK). All spectra reported are shown with minimal smoothing and without background subtraction.

### Mass spectrometry Results and Discussion

Analysis of the intact P-Core complex under conditions where non-covalent interactions are preserved indicated that only one charge state series is present centered at 7000 m/z, which corresponds to a mass of 206148.6Da (Supplementary Figure 1A). This is a difference only of the 0.08% from the theoretical mass of 205989.8Da. The measured masses for the low pH dissociated individual subunits (shown in Supplementary Figure 1b) are close to the theoretical values for  $\alpha$ ,  $\beta 2$  and  $\sigma 2$ , whereas for the  $\mu 2$  subunit a mass of 51055.4 was measured, which corresponds to the theoretical mass of the mono-phosphorylated protein (51051.3 Da). The  $\mu 2$  subunit seems almost completely phosphorylated since we did not observe the charge state series corresponding to the non phosphorylated protein.

MS/MS sequence analysis of tryptic digests of the P-Core and Core demonstrated that phosphorylation occurred in the tryptic peptide 146-162 (data not shown and Fig 1C in main text) and furthermore from studying the fragmentation patterns it was shown that there was only one site of phosphorylation corresponding to Thr156, which is the site of *in vivo* phosphorylation by AAK1 (see Supplementary Fig. 1C and 1D). Analysis of the signal intensities for the 146-162 tryptic peptide from P-Core and Core indicated that the efficiency of phosphorylation was greater than 95% (see supplementary material). This high level of efficiency of phosphorylation is further emphasized by the fact that the ionisation efficiency of phosphorylated peptides in the positive mode are lower than those of the non phosphorylated ones, especially in the presence of other peptides (Bevilaqua et al 2001 : McLachlin et al 2001 : Mann et al 2002). For this reason, measuring the yield of the phosphorylation on the basis of the relative intensity of the signals can be an underestimate (Lawrie et al 2001). Studies on peptide mixtures of known stoichiometry of phosphorylated and non phosphorylated species with a nanoelectrospray source reported that low pH in the positive mode are optimal conditions for the determination of the ratio between the modified and non modified peptides, especially for phosphothreonine containing peptides. However, even in this case an underestimation around 30 % has been detected (Carr et al 1996).

This high stoichiometry of  $\mu 2$ Thr156 phosphorylation was consistent in three independently purified preparations of wild type P-Core that we examined as well as in the phosphorylated mutant forms of the core used in these studies (data not shown). The observation that only the kinase domain of AAK1 is required to obtain virtually complete phosphorylation on only the desired (i.e *in vivo* site) indicates that sufficient peptide substrate specificity determinants required by AAK1 to phosphorylate the  $\mu 2$  subunit of AP2 are contained within the kinase core, which is in line with structural studies on other kinases (Lowe et al 1997) and as predicted by the kinase substrate prediction programme (Brinkworth et al., 2003). *In vivo* additional substrate specificity for the kinase may come from the kinase's localisation in CCPs determined largely by its interaction with clathrin and the  $\alpha$ -appendage of AP2 (Jackson et al., 2003; Conner et al., 2003).

### Supplemental References

Sobott, F., Hernandez, H., McCammon, M.G., Tito, M.A. & Robinson, C.V. (2002) A tandem mass spectrometer for improved transmission and analysis of large macromolecular assemblies. *Anal. Chem.* 74, 1402-7.

Mann, M., Ong, S.E., Gronborg, M., Steen, H., Jensen, O.N. & Pandey, A. (2002) Analysis of protein phosphorylation using mass spectrometry: deciphering the phosphoproteome. *Trends Biotechnol.* **20**, 261-8.

McLachlin, D.T. & Chait, B.T. (2001) Analysis of phosphorylated proteins and peptides by mass spectrometry. *Curr. Opin. Chem. Biol.* **5**, 591-602.

Bevilaqua, L.R., Graham, M.E., Dunkley, P.R., von Nagy-Felsobuki, E.I. & Dickson, P.W. (2001) Phosphorylation of Ser(19) alters the conformation of tyrosine hydroxylase to increase the rate of phosphorylation of Ser(40). *J. Biol. Chem.* **276**, 40411-6.

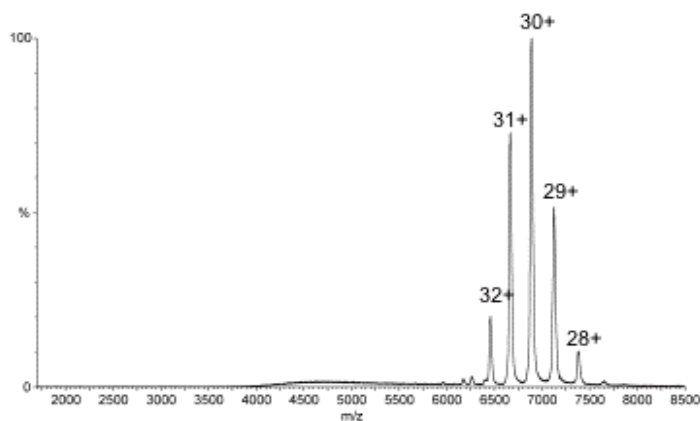
Lawrie, A.M., Tito, P., Hernandez, H., Brown, N.R., Robinson, C.V., Endicott, J.A., Noble, M.E., Johnson, L.N. (2001) Xenopus phospho-CDK7/cyclin H expressed in baculoviral-infected insect cells. *Protein Expr. Purif.* **23**(2), 252-260.

Carr, S.A., Huddleston, M.J. & Annan, R.S. (1996) Selective detection and sequencing of phosphopeptides at the femtomole level by mass spectrometry. *Anal. Biochem.* **239**, 180-92.

Lowe, E.D., Noble, M.E., Skamnaki, V.T., Oikonomakos, N.G., Owen, D.J. and Johnson, L.N. (1997). The crystal structure of a phosphorylase kinase peptide substrate complex: kinase substrate recognition. *Embo J*, **16**, 6646-6658.

Brinkworth, R.I., Breinl, R.A. and Kobe, B. (2003). Structural basis and prediction of substrate specificity in protein serine/threonine kinases. *Proc Natl Acad Sci U S A*, **100**, 74-79.

**A**



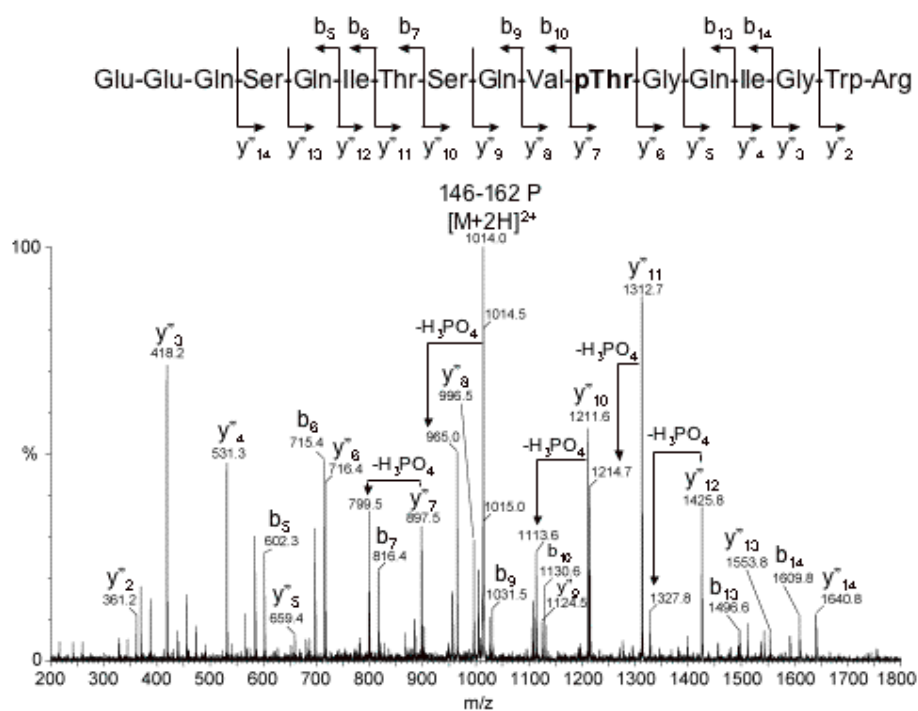
**B**

**Protein**

**Molecular mass (Daltons)**

	Theoretical	Measured
$\alpha$ subunit	70092.2	70099.0 $\pm$ 7.2
$\beta$ 2 subunit	67828.6	67840.0 $\pm$ 3.1
$\mu$ 2-P subunit	51051.3	51055.4 $\pm$ 0.9
$\alpha$ 2 subunit	17017.8	17018.3 $\pm$ 0.2

**C**



D

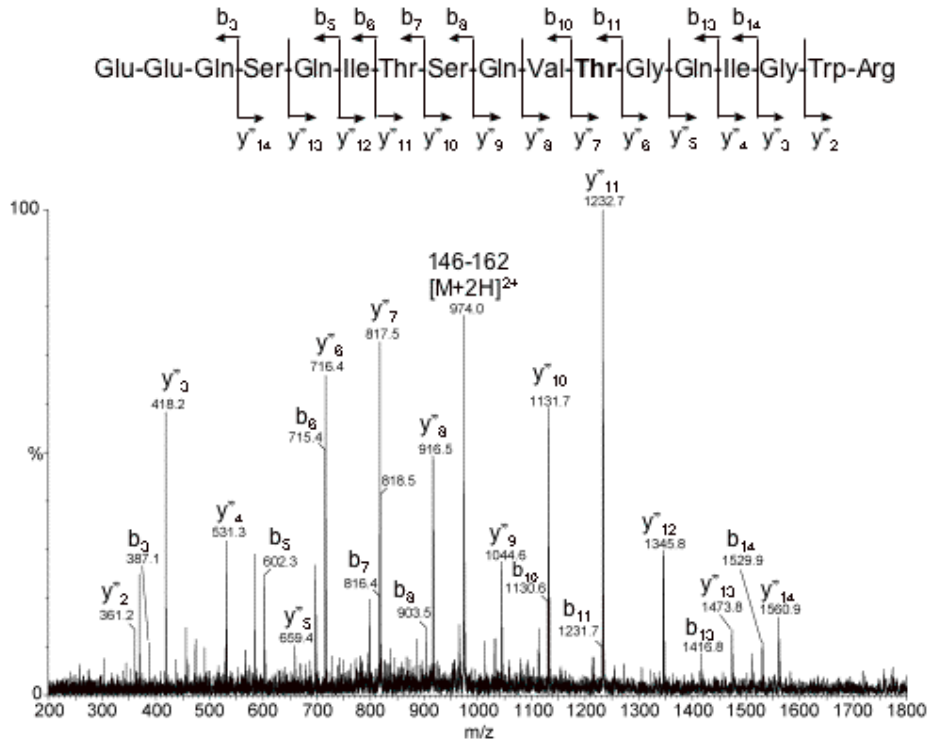


Figure S1

(A) Nano-electrospray mass spectra of the phosphorylated AP2 complex. The intact complex analysed under conditions where non-covalent interactions are preserved. The charge state series of the complex is indicated. Only one charge state series is present centered at 7000 m/z, which corresponds to a mass of 206148.6Da.

(B) Predicted and measured molecular weights of phosphorylated AP2 core subunits

(C) and (D) Sequencing of  $\mu$ 2Thr156 phosphorylation site by analysis of MS/MS fragmentation pattern produced in the tryptic digest of the phosphorylated (C) and non-phosphorylated (D) AP2 cores. In the part of the fragmentation series which does not contain the potentially phosphorylated threonine the two samples show identical fragments, whereas the other part of the series containing Thr156 has a mass difference of 80 between the two spectra, which is the mass corresponding to the addition of a phosphate group. In both the MS/MS spectra the coverage of the sequence is quite high at ~ 70 %: 12 amino acids from 17. Only the identity of the isoleucine residues could not be confirmed due to the fact that isoleucine is isobaric with leucine. (C) MS/MS spectra of the phosphorylated peptide 146-162  $[M+2H]^{2+}$  ion. In the mass spectrum the y" and b ions and the loss of  $H_3PO_4$  (-98Da) on fragmentation are indicated. The corresponding localisation of the product fragments in the sequence of the peptide 146-162 is also shown. (D) MS/MS spectra of the peptide 146-162  $[M+2H]^{2+}$  ion. In the mass spectrum the y" and b ions are indicated. The corresponding localisation of the product fragments in the sequence of the peptide 146-162 is also shown.

## Surface Plasmon Resonance (Biosensor) Supplementary Information

Initial experiments to verify the functionality of recombinant AP2 cores (P-Core and Core) in comparison with the binding of recombinant C- $\mu$ 2 and AP2 isolated from pig brain (as in Fingerhut et al., 2001) were made using the synthetic tail peptide of TGN38 (CKVTRRPKASDYQRL). The peptide was immobilized via the thiol group of its aminoterminal cysteine residue on a carboxy-methylated dextran (CM5) sensor surface using the thiol coupling strategy exactly following the manufacturers instructions (BIAcore AB). After peptide immobilization (~1000RU) the surface was regenerated using pulse injections of 50mM NaOH and 50mM NaOH, 5% SDS to remove non-covalently bound peptide. The subsequent analysis of binding of purified AP2, recombinant AP2 cores or  $\mu$ 2 was carried out exactly as described (Ricotta et al., 2002) except that the running buffer used was 250mM NaCl, 10mM Tris pH8.7 1mM DTT. The binding to a TGN38 peptide in which the critical tyrosine residue was substituted for alanine served as a control and was subtracted before the rate constants were calculated using the Evaluation software supplied by the manufacturer (BIAcore evaluation software, Jonsson et al., 1991). The data obtained (shown in Supplementary Table 1) indicates that the recombinant proteins are at least as functional in their tyrosine-based signal binding as AP2s isolated from intact porcine brain.

	AP2 (pig brain)			AP2 core			AP2 P-core			$\mu$ 2 (157-435)		
	$k_a$ ( $M^{-1} \times s^{-1}$ )	$k_d$ ( $s^{-1}$ )	$K_D$ (nM)	$k_a$ ( $M^{-1} \times s^{-1}$ )	$k_d$ ( $s^{-1}$ )	$K_D$ (nM)	$k_a$ ( $M^{-1} \times s^{-1}$ )	$k_d$ ( $s^{-1}$ )	$K_D$ (nM)	$k_a$ ( $M^{-1} \times s^{-1}$ )	$k_d$ ( $s^{-1}$ )	$K_D$ (nM)
TGN38	$5.1 \times 10^3$	$2.6 \times 10^{-3}$	510	$6.0 \times 10^3$	$2.7 \times 10^{-3}$	450	$8.2 \times 10^4$	$2.9 \times 10^{-3}$	36	$1.1 \times 10^3$	$1.7 \times 10^{-3}$	1,500

Table S1. Rate constants for the binding of purified AP2, recombinant AP2 and  $\mu$ 2 to the sorting signal of TGN38. Analytes were passed over the peptide-derivatized surface for 2 min at 4 concentrations ranging from 100nM to 2 $\mu$ M. The rate constants were calculated from the obtained sensorgrams after subtraction of binding to the mutant control peptide (see above).

The binding to other tail peptides listed below was also tested. As can be seen from Table S2 the various signals were bound with different affinities with the highest being that of TGN38 (450nM) (in line with data obtained from recombinant peptide library screening using recombinant C- $\mu$ 2 (Ohno et al., 1998). The sequences of the sorting signal containing peptides used were derived from the cytoplasmic tails of  
TGN 38 (CKVTRRPKASDYQRL)  
Lamp-1 (CRKRSHAGYQTI)  
LAP (CRMQAQPPGYRHV)  
phosphorylated CD4 (CHRRRQAERM(SP)QIKRLLSEK)  
Limp-II (CRGQGSTDEGTADERAPLIRT)  
Tyrosinase (CKKQPQEERQPLLMDKDDYHSLLYQSHL)

	AP2 (pig brain)			AP2 core			AP2 core (phosphorylated)		
	$K_a$ ( $M^{-1} \times s^{-1}$ )	$K_d$ ( $s^{-1}$ )	$K_D$ (nM)	$K_a$ ( $M^{-1} \times s^{-1}$ )	$K_d$ ( $s^{-1}$ )	$K_D$ (nM)	$K_a$ ( $M^{-1} \times s^{-1}$ )	$K_d$ ( $s^{-1}$ )	$K_D$ (nM)
TGN38	$5.1 \times 10^3$	$2.6 \times 10^{-3}$	510	$6.0 \times 10^3$	$2.7 \times 10^{-3}$	450	$8.2 \times 10^4$	$2.9 \times 10^{-3}$	36
Lamp-1	$3.3 \times 10^3$	$2.5 \times 10^{-3}$	758	$3.5 \times 10^3$	$2.5 \times 10^{-3}$	714	$5.1 \times 10^4$	$2.7 \times 10^{-3}$	53
LAP	$3.0 \times 10^3$	$2.8 \times 10^{-3}$	933	$3.3 \times 10^3$	$2.8 \times 10^{-3}$	848	$4.5 \times 10^4$	$2.9 \times 10^{-3}$	64
Limp-II	$1.5 \times 10^3$	$3.5 \times 10^{-3}$	2,300	$1.8 \times 10^3$	$3.6 \times 10^{-3}$	2,000	$2.0 \times 10^3$	$3.8 \times 10^{-3}$	1,900
Tyrosinase	$2.0 \times 10^3$	$3.2 \times 10^{-3}$	1,600	$2.2 \times 10^3$	$3.3 \times 10^{-3}$	1,500	$2.3 \times 10^3$	$3.4 \times 10^{-3}$	1,500
CD4 (phosphorylated)	$3.0 \times 10^3$	$3.0 \times 10^{-3}$	1,000	$3.3 \times 10^3$	$3.1 \times 10^{-3}$	940	$3.5 \times 10^3$	$3.0 \times 10^{-3}$	857

**Table S2. Binding of purified AP2 and recombinant AP2 core complexes to sorting signals.**

Synthetic peptides corresponding to the sorting signals of the indicated proteins were immobilized on a CM5 sensor surface of a BIAcore 3000 and probed for binding of AP2 purified from pig brain as well as recombinant AP2 core complexes, harboring a phosphorylated or nonphosphorylated Thr156 in the  $\mu 2$  subunit. Binding of purified AP2 was comparable to that of the non-phosphorylated AP2 core, showing the functionality of the recombinant protein. Interestingly, binding to tyrosine sorting signals was enhanced by more than 10-fold upon phosphorylation of  $\mu 2$  at Thr156, while the weak binding of the dileucine signals was almost unaffected.

### Processing of sensorgrams recorded with a BIAcore 3000 biosensor

The binding of AP2 to membranes was recorded in real-time using a BIAcore 3000 biosensor as outlined in Experimental procedures. Before the rate constants for the interaction can be calculated, the original data set has to be processed adequately, which is outlined in the figure below.

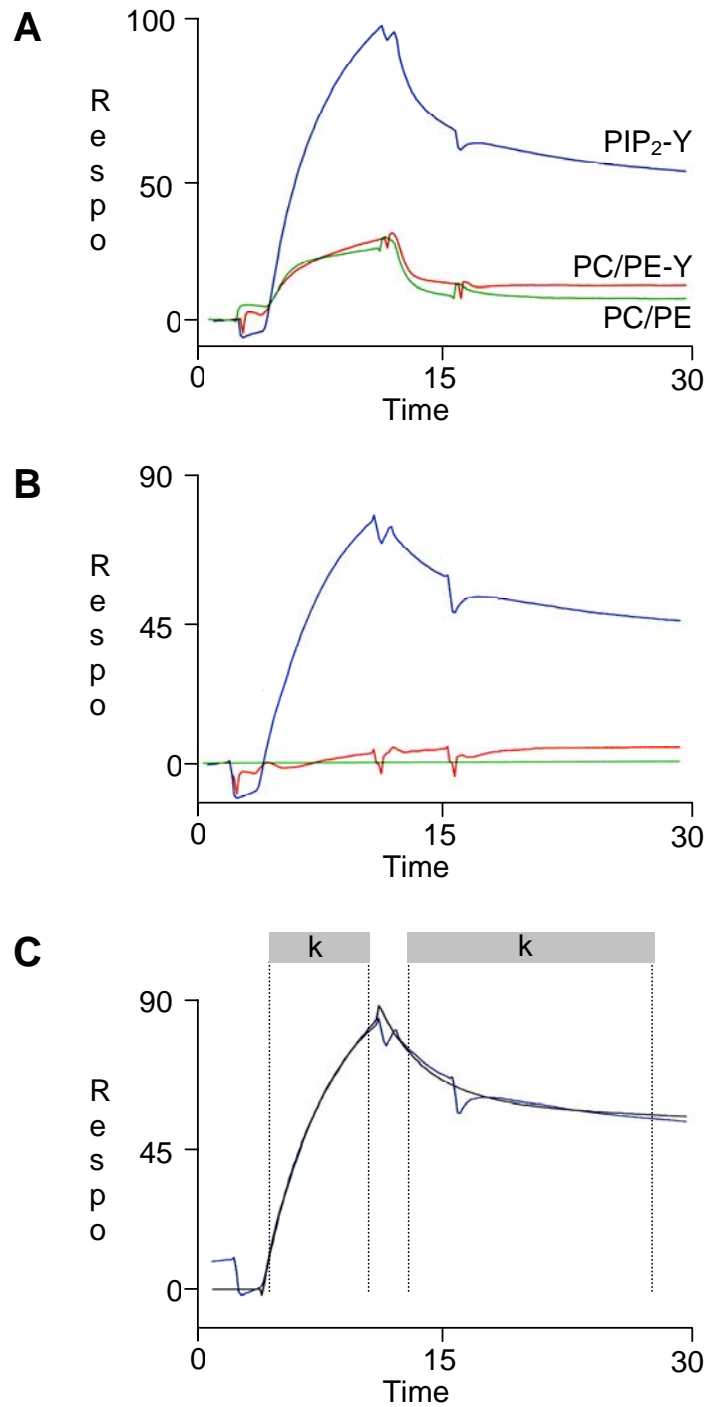




## Figure S2

In **A**, the original data set of binding of recombinant AP2 (non-phosphorylated core) to the 3 indicated surfaces is shown. All 3 sensorgrams were recorded simultaneously in real-time. **B**: After data acquisition, binding of AP2 to membranes containing PC/PE which was regarded as background binding was subtracted from the other two sensorgrams by using the evaluation software supplied by the manufacturer. This resulted in a flat line for PC/PE and a curve very similar to it for PC/PE-Y. Thus, binding of AP2 to PC/PE-Y is negligible. **C**: After background subtraction, the indicated areas of the remaining curve were selected for calculating the rate constants of the interaction ( $k_a$  and  $k_d$ ). The calculation was done by using a mathematical model that assumes 2 binding sites in AP2 for membranes. The significance of the calculated data was verified by superimposition of a theoretical curve (black) with the curve obtained in our experiment (blue). As shown, both curves exhibit a high degree of identity. The visible distortions in the original curve are due to valve switching at the beginning and end of the injection of AP2 that become visible when one of the central parts of the BIAcore biosensor (the integrated fluid cartridge, IFC) reaches the end of its live time.

Fingerhut, A., K. von Figura, and S. Honing. (2001). Binding of AP2 to sorting signals is modulated by AP2 phosphorylation. *J Biol Chem.* 276:5476-82.

Jonsson, U., L. Fagerstam, B. Ivarsson, B. Johnsson, R. Karlsson, K. Lundh, S. Lofas, B. Persson, H. Roos, I. Ronnberg, and et al. (1991). Real-time biospecific interaction analysis using surface plasmon resonance and a sensor chip technology. *Biotechniques.* 11:620-7.